HHS Public Access

Author manuscript

Cancer Immunol Res. Author manuscript; available in PMC 2016 April 01.

Published in final edited form as:

Cancer Immunol Res. 2015 April ; 3(4): 389–398. doi:10.1158/2326-6066.CIR-14-0173.

Three Steps to Breaking Immune Tolerance to Lymphoma: A Microparticle Approach

Amani Makkouk[1], **Vijaya B Joshi**[2], **Caitlin D Lemke**[3], **Amaraporn Wongrakpanich**[2], **Alicia K Olivier**[4], **Sue E Blackwell**[3], **Aliasger K Salem**[2], and **George J Weiner**[1,3]

[1]Interdisciplinary Graduate Program in Immunology, University of Iowa, Iowa City, Iowa, 52242

[2]Department of Pharmaceutical Sciences and Experimental Therapeutics, College of Pharmacy, University of Iowa, Iowa City, Iowa, 52242

[3]Holden Comprehensive Cancer Center and Department of Internal Medicine, Carver College of Medicine, University of Iowa, Iowa City, Iowa, 52242

[4]Department of Pathology, Carver College of Medicine, University of Iowa, Iowa City, Iowa, 52242

Abstract

In situ immunization aims at generating antitumor immune responses through manipulating the tumor microenvironment. Based on recent advances in the understanding of antitumor immunity, we designed a three-step approach to *in situ* immunization to lymphoma: (1) Inducing immunogenic tumor cell death with the chemotherapeutic drug Doxorubicin (Dox). Dox enhances the expression of “eat-me” signals by dying tumor cells, facilitating their phagocytosis by dendritic cells (DC). Due to the vesicant activity of Dox, microparticles (MP) made of biodegradable polymer Poly(lactide-co-glycolide or PLGA can safely deliver Dox intratumorally and are effective vaccine adjuvants; (2) Enhancing T-cell activation using anti-OX40; (3) Sustaining T-cell responses by checkpoint blockade using anti-CTLA-4. *In vitro*, Dox MPs were less cytotoxic to DCs than to B lymphoma cells, did not require internalization by tumor cells, and significantly enhanced phagocytosis of tumor cells by DCs as compared to soluble Dox. In mice, this three-step therapy induced CD4- and CD8-dependent systemic immune responses that enhanced T-cell infiltration into distant tumors leading to their eradication and significantly improving survival. Our findings demonstrate that systemic antitumor immune responses can be generated locally by three-step therapy and merit further investigation as an immunotherapy for lymphoma patients.

Keywords

Cancer immunotherapy; biodegradable microparticles; Doxorubicin; anti-CTLA-4; anti-OX40; *in situ* immunization

Corresponding Author: George J Weiner, Holden Comprehensive Cancer Center at The University of Iowa, 5970Z JPP, University of Iowa, Iowa City, IA 52242; Phone: 319.353.8620; Fax: 319.353.8988; george-weiner@uiowa.edu.

Conflict-of-interest: The authors declare no competing interests.

Introduction

The goal of many forms of cancer immunotherapy is to overcome immunologic tolerance to tumor antigens and generate immune responses in the form of effector T cells (1). *In situ* immunization is attractive because it utilizes the patient's unique tumor antigens by inducing tumor cell death *in situ.* This limits systemic drug toxicity and provides dendritic cells (DC) with a wide selection of tumor antigens to be presented to antigen-specific T cells (2, 3).

Recent advances in our understanding of antitumor immunity suggest generating a potent, long-lasting antitumor response might benefit from a three step approach. Step One - treatment would be delivered locally to induce tumor cell death and provide tumor antigens to DCs. Step Two - activation of tumor-specific T cells by DCs would be enhanced. Step Three - the activated T-cell response would be maintained so the systemic response can proceed unrestrained (2).

Doxorubicin (Dox) is an excellent candidate drug for enhancing tumor antigen uptake by DCs, and is routinely used for lymphoma (4). Dox induces immunogenic cell death which stimulates an immune response in part by inducing surface expression of calreticulin, an "eat-me" signal that enhances phagocytosis of dying tumor cells by DCs (5–7).

In order for T cells to be activated by DCs, they must also receive a costimulatory signal, which can be supplied by toll-like receptor (TLR) agonists (such as TLR9 agonist CpG), cytokines (such as IL2) and stimulatory antibodies that target members of the tumor necrosis factor receptor (TNFR) superfamily (such as OX40) (8–10). OX40 augments T-cell function and survival (10–12). A stimulatory antibody that activates OX40 (anti-OX40) could thus be used to further activate tumor-specific T cells. We chose to focus on anti-OX40 due to its demonstrated synergistic activity with anti-CTLA-4, which enhances antitumor immune responses in murine lymphoma models (13).

The activity of T cells is tightly regulated by checkpoints that control the magnitude of the immune response, exemplified by cytotoxic T-lymphocyte antigen 4 (CTLA-4). CTLA-4 is upregulated on activated T cells, and signaling via CTLA-4 reduces T-cell proliferation and activity (14). In addition, CTLA-4 plays a central role in the suppressive effect of regulatory T cells (Treg) (15). This provides strong rationale for including checkpoint blockade as a final step of *in situ* immunization.

While the use of Dox to induce immunogenic cell death is attractive for *in situ* immunization, an intratumoral injection of the soluble drug is not feasible due to its potent vesicant effects (16). Poly(lactide-co-glycolide) or PLGA is an FDA-approved biodegradable polymer that is clinically used in surgical sutures and for controlled delivery of therapeutic drugs (17). Following intratumoral injection, PLGA microparticles (MP) can provide sustained release of encapsulated molecules (18) into the tumor microenvironment without a vesicant effect. In addition, PLGA MPs are effective vaccine adjuvants. They activate the NALP3 inflammasome in DCs, which leads to IL1β secretion and the enhancement of innate and antigen-specific cellular immune responses (19).

Based on this background, we hypothesized that a three-step approach to *in situ* immunization (Dox MPs given intratumorally combined with systemic anti-CTLA-4 and anti-OX40) can elicit a systemic curative adaptive immune response.

Materials and Methods

Mice and Cell Lines

Mice (BALB/c and C57BL/6 females, 6–8 weeks old) were purchased from Harlan Laboratories (Indianapolis, IN). All animal protocols were approved by the Institutional Animal Care and Use Committee at the University of Iowa and complied with NIH Guidelines.

A20 (murine BALB/c B-cell lymphoma), Raji (human Burkitt lymphoma B), and EL4 (murine C57BL/6 T-cell lymphoma) were purchased from American Type Culture Collection (ATCC, Manassas, VA). Epstein-Barr virus (EBV)-transformed B cells were previously generated per standard protocols (20, 21). Subject informed consent was obtained in accordance with the Declaration of Helsinki under protocols approved by the institutional review board. Cells were cultured in RPMI-1640 medium (Gibco, Carlsbad, CA) supplemented with 10% heat-inactivated FCS (HyClone, Logan, UT), 100 U/mL penicillin, 100 μg/mL streptomycin, and 50 μM 2-ME (Gibco). All cell lines used were confirmed to be Mycoplasma free. No additional validation assays were performed.

Therapeutic Antibodies

Anti-CTLA4 (hamster IgG, clone UC10-4F10-11) and anti-OX40 (rat IgG1, clone OX86) were purchased from BioXCell (West Lebanon, NH). A20 were previously shown to lack surface expression of CTLA-4 and OX40 (13).

Generation of DCs

To generate murine bone-marrow-derived DCs, bone marrow cells were flushed from tibias and femurs of BALB/c mice, and mononuclear cells isolated using Ficoll gradient separation (Fico/Lite-LM, Atlanta Biologicals, Flowery Branch, GA). Cells were cultured in medium supplemented with 20 ng/mL each GM-CSF and IL4 (PeproTech, Rocky Hill, NJ) for 7 days. Non-adherent cells were harvested. Cells were > 70% DCs as determined by CD11c staining.

Viability Assays

The MTS assay for viability was used to determine the cytotoxic activity of Dox MPs against A20 and DCs (Promega, Madison, WI). Briefly, 5×10^3 A20 cells or DCs were incubated with Dox MPs (8 μg/mg) for 24, 48 or 72 h (4 wells per group) at a range of Dox concentrations. Blank MPs were used as negative controls. MTS was added for 4 h at 37°C. Following centrifugation, 90 μl of supernatant was removed. Absorbance was read at 490 nm using a Thermomax Microplate Reader (Molecular Devices, Sunnyvale, CA).

Rhodamine Particle Uptake

Uptake of particles by A20 and DCs was determined using rhodamine-loaded MPs prepared similarly to Dox MPs. A20 and DCs were incubated for 24 h either alone or in a 1:1 mix with rhodamine-loaded MPs (0.5 μg/mL). Cells were washed and stained for CD11c –APC-Cy7 and CD19-APC (BD Biosciences (BD), San Jose, CA). Uptake was assessed by flow cytometry using LSR II flow cytometer (BD) by gating on rhodamine$^+$ DCs (CD11c$^+$) and A20 (CD19$^+$).

Transmission Electron Microscopy

Uptake of Dox MPs was assessed using transmission electron microscopy (TEM). Briefly, A20 and DCs were incubated for 24 h with Dox MPs (1 μg/mL) or blank MPs (equivalent weight), washed with PBS and fixed in 2.5% glutaraldehyde in 0.1 M sodium cacodylate. Post-fixation was carried out in 1% osmium tetroxide with 1.5% potassium ferrocyanide for 2 hours, 2.5% uranyl acetate for 20 minutes, followed by dehydration in graded ethanol and embedding in Epon resin (Electron Microscopy Sciences, Hatfield, PA). Ultrathin sections were counterstained with uranyl acetate and lead citrate. TEM images were taken by JEOL JEM-1230 transmission electron microscope provided with Gatan UltraScan 1000 2k × 2k CCD camera (JEOL USA, Inc., Peabody, MA). Micrographs were processed with ImageJ Software.

Phagocytosis Assay

A20 phagocytosis was quantified using A20 cells labeled with CellTrace Violet (Invitrogen, Carlsbad, CA). Labeled A20 were left untreated or treated with Dox MPs for 48 h (3 wells per group) at various concentrations. Controls included soluble Dox (at the same concentrations) and blank MPs (at equivalent weights). Treated A20 were washed and co-incubated with DCs at a 1:1 ratio for 2 h, stained with anti-CD11c-APC-Cy7 (BD), and analyzed by flow cytometry. The percentage of double-positive cells (CD11c and CellTrace Violet) was determined.

Confocal Microscopy

MP uptake by A20 cells was visualized by culturing cells for 24 h with Dox MPs at a final Dox concentration of 2.25 μg/mL. Cells were washed, incubated at 37°C for 2 h with the nucleic acid dye Cyto16 (Invitrogen), washed, fixed, cytospun and mounted on Vectashield (Vector Laboratories, Burlingame, CA). DCs cultured on dishes with cover slide bottoms were treated for 3 h together with Cyto-16, then stained with anti-CD11c-APC (BD) for 2 h (4°C) and visualized. Images were acquired with a Zeiss LSM510 confocal microscope (Carl Zeiss Co., Germany) equipped with a 63× oil-immersion objective and controlled by ZEN 2009 software (Zeiss). Images were processed with ImageJ Software.

In Vivo A20 Tumor Transplantation and Assessment

BALB/c mice were subcutaneously inoculated with A20 at a dose of 6.7–9 × 10^6 A20 cells in 100 μL sterile PBS on the right and left flanks. Treatment began when tumors reached 5–7 mm in largest diameter (days 6–11 post inoculation). Tumor growth was monitored by

calipers and expressed as length by width in square millimeters. Mice were euthanized when either tumor reached 20 mm in any direction or when tumor sites ulcerated.

A20 Tumor Immunotherapy

Dox MPs (2 μg Dox in 100 μL PBS) or PBS (100 μL) were injected into the left flank tumor. Three doses of anti-CTLA-4 and anti-OX40 (collectively referred to as Ab) were administered by intraperitoneal injections every 3–4 days. Half the published doses were used (13): 50 μg for anti-CTLA-4 and 200 μg for anti-OX40 per injection. Treatment groups included PBS, PBS+anti-CTLA-4, PBS+anti-OX40, Dox MP, Dox MP+anti-CTLA-4, Dox MP+anti-OX40 and Dox MP+anti-CTLA-4+anti-OX40. Mice were treated and monitored as before. Additional studies were done with mice receiving lower doses of Ab.

CD4 and CD8 Depletion

Anti-CD4 (rat IgG2b, clone GK1.5) and anti-CD8 (rat IgG2b, clone 2.43) were purchased from BioXCell (West Lebanon, NH). Rat IgG (MP Biomedicals LLC, Santa Ana, CA) was used as isotype control. Antibodies (200 μg per injection) were administered one day before therapy and on Days +1, +4, +8, +12 and +18. CD4 and CD8 T-cell depletion was validated by flow cytometry (>99% depletion).

Flow Cytometric Analysis of Tumors and Lymphoid Tissue

Tumor and lymph node immune infiltrates were evaluated on Day 5 post therapy. Injected tumors, contralateral tumors and draining lymph nodes were harvested and single-cell suspensions surface stained with CD3-APC, CD4-FITC, CD8-PE-Cy7, IFNγ-PE, CD11b-PE, CD11c-APC-Cy7, CD44-APC, CD62L-PE (BD), Foxp3-APC and Gr-1-FITC (eBioscience, San Diego, CA) and fixed using BD Cytofix/Cytoperm.

Statistical Analysis

GraphPad Prism software, version 6.0 (San Diego, CA) was used to analyze tumor growth and to determine differences between groups using unpaired 2-tailed Student t tests or ANOVA (Bonferroni correction) where appropriate. Survival curves were compared using the log-rank (Mantel-Cox) test.

Supplemental methods are detailed in the online data supplement

Results

Dox MPs provide sustained release of Dox

Dox MPs were prepared by the double emulsion solvent evaporation method (22) (Supplementary Figure 1A). The target particle size was 1 μm based on ability to promote inflammasome activation in DCs (19). Scanning electron microscopy revealed a smooth morphology and spherical shape (Supplementary Figure 1B). Particle size was 1.2 ± 0.4 μm, which is comparable to the size of blank MPs (empty MPs) of 1.4 ± 0.3 μm. Kinetic release studies showed 13 % burst release of Dox within one hour followed by sustained release as the polymer underwent degradation (Supplementary Figure 1C).

Dox MPs kill tumor cells more slowly than soluble Dox and are less cytotoxic to DCs

Dox MPs and soluble Dox were compared for their ability to kill A20 lymphoma cells. Increasing concentrations of soluble Dox led to a significant decrease in A20 viability within 24 h of exposure (87% at 0.5625 μg/mL versus 46% at 1.125 μg/mL on Day 1; $p < 0.0001$) (Figure 1A). A less pronounced decrease in A20 viability was seen with Dox MPs (97% at 0.5625 μg/mL versus 84% at 1.125 μg/mL Dox on Day 1; not statistically significant). This was confirmed when comparing Dox MPs to soluble Dox (46% with soluble Dox versus 84% with Dox MPs at 1.125 μg/mL; $p < 0.0001$) and also after 48 h exposure (5% with soluble Dox versus 24% with Dox MPs at 1.125 μg/mL on Day 2; $p < 0.0001$). These data indicate that Dox MPs kill A20 cells more slowly than soluble Dox. Moreover, tumor cells had an average survival of 82% following three days of incubation with blank MPs, indicating that PLGA MPs are not toxic to tumor cells.

Upon injection into the tumor microenvironment, both tumor cells and immune cells would be exposed to Dox released from degrading MPs. Therefore, we evaluated the effect of Dox MPs and soluble Dox on DCs. Dox MPs were less cytotoxic to DCs than to A20 (24 h survival at 1.125 μg/mL Dox - 23% for A20 versus 81% for DCs; $p < 0.05$). On the other hand, soluble Dox was equally cytotoxic to both (26% survival for A20 versus 19% for DCs; not statistically significant) (Figure 1B). By 72 h, lower concentrations of Dox MPs were still significantly more cytotoxic to A20 than to DCs (0% survival for A20 versus 74% for DCs at 0.28125 μg/mL; $p < 0.001$), while higher concentrations were cytotoxic to both (0% survival for A20 versus 10% for DCs at 2.25 μg/mL; not statistically significant). This suggests careful titration of Dox MP doses will be important to identify the window where Dox MPs are toxic to malignant cells but not to DCs in the tumor.

Dox MPs are cytotoxic despite limited internalization

To evaluate whether MPs are internalized by cells, we utilized rhodamine-labeled MPs and tracked their uptake by tumor cells and DCs by flow cytometry (Figure 2A). A20 tumor cells did not internalize MPs, which is in agreement with published reports (23). In contrast, DCs readily took up the particles even when cocultured with tumor cells. Similar results were found with Dox MPs taking advantage of the natural fluorescence of Dox (24) (Figure 2B).

Internalization and cytotoxicity were not strongly linked. A20 tumor cells incubated with Dox MPs showed signs of cytotoxicity (dissolution of cellular organelles, increased chromatin clumping and nuclear fragmentation, and blebbing of nuclear and plasma membranes) despite limited internalization while DCs readily took up MPs (red arrows) but showed little toxicity (Figure 2C). Collectively, these data show that Dox MPs do not require internalization for their cytotoxic activity but rather release the encapsulated drug locally, which is then taken up by tumor cells. In addition, various cells in the tumor microenvironment can have different levels of sensitivity to the slow release of Dox by the MPs.

Dox MPs enhance phagocytosis of tumor cells by DCs

We next evaluated whether Dox MPs enhance phagocytosis of tumor cells by DCs in a manner similar to that seen with soluble Dox (7). Increasing concentrations of Dox enhanced phagocytosis of A20 cells treated with both soluble Dox and Dox MPs. However, Dox MPs were superior to soluble Dox at all concentrations tested ($p < 0.001$) (Figure 3A). Phagocytosis was also visualized by confocal microscopy (Supplementary Figure 2). Together, these results show that Dox MPs are superior to soluble Dox in inducing phagocytosis of tumor cells by DCs.

Dox MPs exert similar effects to soluble Dox in human cell lines

We also evaluated the effect of Dox MPs on human cell lines using Dox concentrations comparable to peak plasma concentrations achieved in lymphoma patients (278 ng/mL at 30 mg/m^2 Dox) (25). Dox MPs were similar to soluble Dox in their killing efficiency of EBV-transformed and Raji B cells (Supplementary Figure 3A). Dox MPs were also similar to soluble Dox at inducing the phagocytosis of EBV-transformed B cells by autologous myeloid-derived dendritic cells (MDDC) when EBV-transformed B cells and MDDCs were simultaneously incubated with Dox or Dox MPs (Supplementary Figure 3B, C).

Three-step therapy eradicates distant tumors and enhances survival

To examine the induction of systemic immune responses, we utilized a two-tumor lymphoma model similar to that established by Houot and colleagues (13). Mice were inoculated subcutaneously with A20 cells on both flanks, with one site used for *in situ* immunization (injection of Dox MPs) and the contralateral site observed to assess the systemic antitumor response. In this model, regression of the contralateral tumor can only be due to systemic immune responses.

We first evaluated the effect of Dox MP alone. No mice receiving Dox MPs showed any signs of skin ulceration/necrosis even at doses as high as 100 μg Dox, confirming that the sustained release properties of the MPs protect mice from the vesicant effect of Dox. While local tumors regressed following treatment with intratumoral Dox MPs, no systemic antitumor response was observed (as measured by regression of contralateral tumors). We then evaluated the combination of Dox MPs plus antibody therapy. Mice received a single intratumoral injection of Dox MPs and three systemic injections of anti-CTLA-4 and anti-OX40 (collectively referred to as Ab). Control group mice received intratumoral PBS with or without Ab. Initial studies revealed that systemic immune responses were not generated when Dox MPs were used at a dose of 100 μg Dox. Dose titration revealed systemic antitumor responses were generated with a lower dose of Dox MPs (2 μg) (Figure 4), in agreement with our *in vitro* data demonstrating high doses of Dox MPs are detrimental to both tumor cells and DCs. These data also demonstrate that the systemic antitumor response is not due to systemic release of Dox into the circulation, which would have resulted in a greater therapeutic effect on the contralateral tumor with higher doses of Dox MPs.

Mice treated with the optimized dose of Dox MPs (2 μg Dox) combined with Ab had significantly enhanced tumor-free survival as compared to mice receiving Ab therapy only (87% versus 67%; $p < 0.05$) (Figure 4A). This therapy generated a potent systemic immune

response that eradicated most of the contralateral tumors (Figure 4A, B). Mice that received Dox MP+Ab and became tumor-free were re-challenged with 10 million A20 tumor cells implanted subcutaneously at a different site from the MP-injected tumor at Day 51 post tumor-challenge (n=5). These mice remained tumor-free demonstrating a long-term memory response (data not shown).

Three-step therapy induces CD4- and CD8-dependent immune responses and requires all therapy components for maximum efficiency

We next evaluated the contributions of the various components of therapy. Dox MPs alone were incapable of inducing efficient immune responses, as indicated by unrestrained growth of contralateral tumors (Figure 5A) and poor survival (Supplementary Figure 4). Similarly, anti-CTLA-4 alone or in combination with Dox MPs was insufficient to cure contralateral tumors. While anti-OX40 alone initially delayed tumor growth, tumors progressed with time and survival was not enhanced beyond 30% even when combined with Dox MPs ($p > 0.05$; Supplementary Figure 4). In contrast, all three components significantly reduced tumor growth as compared to all other groups (6 out of 8 mice became tumor-free) (Figure 5A), confirming all components are needed for maximum efficacy.

We further examined the dose of Ab used in three-step therapy (referred to as Full Dose) by comparing it to Ab doses that were $1/4^{th}$ and $1/16^{th}$ the established dose (Supplementary Figure 5). Efficacy was reduced with both lower doses, confirming that our established Ab dose (which is 50% of the reported dose (13)) was optimal in this model.

To confirm the role of T-cell subsets in the therapeutic response, CD4 or CD8 T cells were depleted. Depletion of either CD4 or CD8 T cells abolished the therapeutic effect (Figure 5B), confirming that the systemic antitumor effect was T cell-mediated.

Three-step therapy enhances T-cell infiltration into contralateral tumors

We next evaluated the tumor microenvironment histologically five days after initiation of therapy (Supplementary Figure 6). While all tumors showed necrosis, mice that received Ab therapy had significantly more tumor necrosis than PBS control mice. Dox MP+Ab therapy and Ab therapy alone induced comparable necrosis, suggesting that the necrosis seen was due to antibody therapy rather than Dox MPs.

While Dox MP+Ab had no detectable effect on necrosis in the contralateral tumor, it did impact on T-cell infiltration (Figure 6). Mice treated with Dox MP+Ab had an increased percent of T cells infiltrating contralateral tumors. While CD4 T-cell infiltration was significantly enhanced, CD8 T cells showed a trend towards enhancement. These data are in agreement with T-cell depletion data indicating a therapeutic response is T cell-dependent. A lower percentage of T cells was seen in the injected tumors, suggesting that Dox MPs could be cytotoxic to T cells and eliminated them locally. Alternatively, the low percent of T cells in the injected tumor could be due to systemic trafficking.

We also examined Tregs, DCs, and myeloid-derived suppressor cells within tumors and found no differences between three-step therapy and Ab therapy (Supplementary Figure 7). Evaluation of T cells and their activation phenotype (CD44 and CD62L expression) in

draining lymph nodes of both local and contralateral tumors on Day 7 post therapy similarly revealed no significant differences between the two groups (Supplementary Figures 8 and 9).

As illustrated in Figure 1, DC viability dropped after 3 days of incubation *in vitro* with Dox MPs. Many factors, including retention of Dox in the media, could have impacted on this. We therefore evaluated the effect of Dox MPs on DC viability *in situ*, and found that it was not affected as indicated by the similar percentages of DCs infiltrating Dox MP-injected tumors and contralateral tumors (Supplementary Figure 7).

Various approaches to evaluating the cytotoxic T-cell response were assessed, including interferon gamma (IFNγ) assays by ELISpot and flow cytometry, CD107a surface expression, and IL2 production. Evaluation of IFN γ responses by flow cytometry proved most reproducible. Antigen-specific T-cell responses were examined by flow cytometry in the spleens and draining lymph nodes on Day 7 post therapy by incubating cell suspensions overnight with irradiated A20 tumor cells. The percentage of IFNγ-producing CD8 T cells was similar with three-step therapy and Ab therapy (Supplementary Figure 10).

Three-step therapy is effective in a murine EL4 lymphoma tumor model

The ability of Dox MPs to enhance the effect of Ab therapy was also evaluated in the EL4 T-cell lymphoma model. Our prior studies demonstrated MPs containing higher doses of Dox are needed to effectively treat EL4, and that EL4 grows too rapidly for a two-sided model to be valuable (26). We therefore evaluated the effect of three-step therapy on EL4 by treating a single tumor with Dox MPs at a dose of 25 μg Dox. Using this approach, Dox MP +Ab significantly reduced EL4 tumor burdens and resulted in 50% long-term survival. None of the mice receiving Ab therapy alone survived (Supplementary Figure 11).

Discussion

With the growth of scientific insight into pathways that regulate the immune system and cancer, we can now more intelligently design and combine immunotherapies that work in different ways to overcome deficiencies of single therapies (27). One attractive approach is to use *in situ* therapy with MPs to manipulate the tumor microenvironment in a manner that breaks tolerance and allows development of a robust immune response. The number of variables that needs to be evaluated when trying to optimize the promise of such a multistep approach is considerable. Here, we address many of these variables, and demonstrate this approach has promising immunologic and therapeutic effects.

An ideal *in situ* immunization approach would deliver localized and effective drug concentrations into the tumor with low systemic toxicity (23). Given its long history of FDA-approved use for biomedical applications and its biocompatibility (28), PLGA was seen as an excellent candidate polymeric vehicle for controlled release of Dox from MPs into the tumor.

We first optimized formulation parameters affecting particle size, loading, and release. 1-μm PLGA MPs have been shown to be more effective than 200 nm, 500 nm, and 5-μm particles

as vaccine adjuvants (29). The relatively low dose of Dox MPs, coupled with their sustained release, proved to be a safe combination for DCs that survived well *in vitro* and *in situ* despite internalizing the particles.

A20 tumor cells were killed more slowly by Dox MPs than by soluble Dox, as previously seen with chemotherapy-loaded PLGA particles (23). However, Dox MPs resulted in more efficient phagocytosis. Dox MPs and soluble Dox were compared based on equivalent *total* amounts of Dox. However, at any given time point and at equivalent "doses", the amount of Dox released by Dox MPs was likely lower than that of soluble Dox. As such, one explanation for why Dox MPs were superior to soluble Dox is that the exposure of malignant cells to a lower Dox concentration enhanced the expression of calreticulin as compared to the bolus dose of soluble Dox (30). Because of technical difficulties associated with Dox MPs adhering to tumor cells, we were unable to demonstrate that Dox MPs calreticulin expression by tumor cells. Shurin and colleagues have shown that ultra-low concentrations of Dox regulate the activity of small Rho GTPases that control the endocytic activity of DCs (31).Thus, it is also possible that Dox MPs adherent to Dox MP-treated A20 cells may be contributing to the enhanced phagocytosis by exposing DCs to very low concentrations of Dox.

Three-step therapy was superior to Ab therapy in inducing curative immune responses. The depletion of CD4 and CD8 T cells abrogated the therapeutic immune response, indicating that it was T cell-mediated. Several studies have confirmed the role of CD8 T cells in Dox-mediated antitumor immune responses (32, 33) and of both CD4 and CD8 T cells in anti-CTLA-4- and anti-OX40-mediated immune responses (13, 34, 35). Thus, the finding that both CD4 and CD8 cells are needed for an optimal antitumor effect in our studies was not surprising.

To investigate how the addition of Dox MPs to Ab therapy is modulating the intratumoral T-cell response, we examined the Treg population and found no effect of three-step therapy on the percent of Tregs. On the other hand, we found enhanced CD4 T-cell infiltration in contralateral but not injected tumors. These results suggest changes induced by therapy enhanced the ability of CD4 T cells to contribute to the immune response and overcome effects of Tregs.

The combination of Dox MPs, anti-CTLA-4 and anti-OX40 was required for the most efficient immune response. Given that Dox MPs alone were incapable of generating immune responses and the combination of anti-CTLA-4 and anti-OX40 without Dox MPs was not as efficient at reducing tumor burden as three-step therapy, it is likely that anti-OX40 is amplifying the primed T-cell response generated with Dox MPs and that anti-CTLA4 is allowing for that response to be maintained. This contention is supported by enhanced T-cell infiltration in tumors following the three components as compared to Ab therapy.

The increase in pathologically-detectable destruction of established tumors, as reflected by tumor necrosis, was seen with both the three-step therapy and Ab therapy. Quantifying necrosis within a tumor sample is difficult, and it was not possible to determine definitively whether three-step therapy enhanced necrosis, however the improved overall outcome

suggests this is the case. Similar responses were seen in tumor samples from patients receiving immunotherapy, and may thus be reflective of the ongoing antitumor immune response (36).

We also validated the efficiency of three-step therapy in the EL4 tumor model. There are clear differences between mouse models of malignancy such as A20 or EL4 and human tumors. An example is potential retroviral contamination of cell lines that could serve as target antigens. Irrespective of the target antigen or immunogenicity of the model, our studies demonstrate that *in situ* treatment with Dox MPs can enhance the immunotherapy effects of immunostimulatory and checkpoint blockade Abs. Further studies will be needed to assess the efficacy of our design in other tumor models in mice, and eventually in clinical trials.

The three-step design is complex, and the number of agents that could be evaluated for each step is extensive. Other approaches, such as local radiation, can be used to induce local immunogenic cell death (37). Anti-OX40 can be substituted with other immunostimulatory antibodies targeting TNFR co-stimulatory molecules, including CD40 and CD137 or TLR agonists such as CpG (37). Anti-CTLA-4 can be substituted with other antibodies that mediate checkpoint blockade such as anti-PD-1 (38). Alternatives related to the dosing and timing of how these agents could be used together leads to an almost endless number of possible combinations. The studies reported here highlight the value of the three-step approach rather than demonstrate that the specific agents or regimen used is superior to other regimens.

Indeed, given that Dox MPs are not clinically approved, a faster translation to the clinic could require approximation of our design using readily-available reagents such as liposomal Dox (Doxil®). In preliminary studies, we found Dox MPs were more effective than liposomal Dox in inducing systemic immune responses in mice (data not shown) which is why they were used. PLGA particles were shown to be superior to liposomal formulations in inducing cellular immune responses, which was attributed to their sustained release rather than an adjuvant effect of the synthesizing material (39). Indeed, liposomal Dox is currently under consideration for a clinical trial exploring a combination similar to that outlined in this report. While liposomal Dox would provide a more direct path toward clinical evaluation, studies comparing Dox MPs to liposomal Dox in human cell lines would also be informative.

In conclusion, recent advances in our understanding of cancer immunotherapy suggest rational combined approaches will be keys to enhancing efficacy. We evaluated a three-step approach to *in situ* immunization using biodegradable Dox MPs, anti-CTLA-4 and anti-OX40 (Figure 7). Further preclinical evaluation of this promising therapeutic strategy in other types of cancer is ongoing, as are plans to translate these findings to the clinic.

Supplementary Material

Refer to Web version on PubMed Central for supplementary material.

Acknowledgements

We thank Sean Geary for help with tumor freezing, Justin Fishbaugh of the Flow Cytometry Facility, and Chantal Allamargot and Katherine Walters of Central Microscopy Research Facility.

Financial Support: This work was supported by grants from the National Cancer Institute at the National Institutes of Health (P50 CA97274/ UI Mayo Clinic Lymphoma SPORE grant and P30 CA086862 Cancer Center support grant).

References

1. Topalian SL, Weiner GJ, Pardoll DM. Cancer immunotherapy comes of age. J Clin Oncol. 2011; 29:4828–4836. [PubMed: 22042955]
2. Mellman I, Coukos G, Dranoff G. Cancer immunotherapy comes of age. Nature. 2011; 480:480–489. [PubMed: 22193102]
3. Crittenden MR, Thanarajasingam U, Vile RG, Gough MJ. Intratumoral immunotherapy: using the tumour against itself. Immunology. 2005; 114:11–22. [PubMed: 15606790]
4. Visani G, Isidori A. Doxorubicin variants for hematological malignancies. Nanomedicine. 2011; 6:303–306. [PubMed: 21385131]
5. Vacchelli E, Galluzzi L, Fridman WH, Galon J, Sautes-Fridman C, Tartour E, et al. Trial watch: Chemotherapy with immunogenic cell death inducers. Oncoimmunology. 2012; 1:179–188. [PubMed: 22720239]
6. Locher C, Conforti R, Aymeric L, Ma Y, Yamazaki T, Rusakiewicz S, et al. Desirable cell death during anticancer chemotherapy. Ann New York Acad Sci. 2010; 1209:99–108. [PubMed: 20958322]
7. Obeid M, Tesniere A, Ghiringhelli F, Fimia GM, Apetoh L, Perfettini JL, et al. Calreticulin exposure dictates the immunogenicity of cancer cell death. Nat Med. 2007; 13:54–61. [PubMed: 17187072]
8. Vacchelli E, Galluzzi L, Eggermont A, Fridman WH, Galon J, Sautes-Fridman C, et al. Trial watch: FDA-approved Toll-like receptor agonists for cancer therapy. Oncoimmunology. 2012; 1:894–907. [PubMed: 23162757]
9. Vacchelli E, Galluzzi L, Eggermont A, Galon J, Tartour E, Zitvogel L, et al. Trial Watch: Immunostimulatory cytokines. Oncoimmunology. 2012; 1:493–506. [PubMed: 22754768]
10. Wolchok JD, Yang AS, Weber JS. Immune regulatory antibodies: are they the next advance? Cancer J. 2010; 16:311–317. [PubMed: 20693841]
11. Aguilar LK, Guzik BW, Aguilar-Cordova E. Cytotoxic immunotherapy strategies for cancer: mechanisms and clinical development. Journal of cellular biochemistry. 2011; 112:1969–1977. [PubMed: 21465529]
12. Hollander N. Immunotherapy for B-cell lymphoma: current status and prospective advances. Front Immunol. 2012; 3:3. [PubMed: 22566889]
13. Houot R, Levy R. T-cell modulation combined with intratumoral CpG cures lymphoma in a mouse model without the need for chemotherapy. Blood. 2009; 113:3546–3552. [PubMed: 18941113]
14. Grosso JF, Jure-Kunkel MN. CTLA-4 blockade in tumor models: an overview of preclinical and translational research. Cancer Immunity. 2013; 13:5. [PubMed: 23390376]
15. Pardoll DM. The blockade of immune checkpoints in cancer immunotherapy. Nat Rev Cancer. 2012; 12:252–264. [PubMed: 22437870]
16. Conde-Estevez D, Mateu-de Antonio J. Treatment of anthracycline extravasations using dexrazoxane. Clin Transl Oncol. 2014; 16:11–17. [PubMed: 23949792]
17. Danhier F, Ansorena E, Silva JM, Coco R, Le Breton A, Preat V. PLGA-based nanoparticles: an overview of biomedical applications. J Control Release. 2012; 161:505–522. [PubMed: 22353619]
18. Houot R, Goldstein MJ, Kohrt HE, Myklebust JH, Alizadeh AA, Lin JT, et al. Therapeutic effect of CD137 immunomodulation in lymphoma and its enhancement by Treg depletion. Blood. 2009; 114:3431–3438. [PubMed: 19641184]

19. Sharp FA, Ruane D, Claass B, Creagh E, Harris J, Malyala P, et al. Uptake of particulate vaccine adjuvants by dendritic cells activates the NALP3 inflammasome. Proc Natl Acad Sci U S A. 2009; 106:870–875. [PubMed: 19139407]
20. Tosato, G.; Cohen, JI. Generation of Epstein-Barr Virus (EBV)-immortalized B cell lines. In: Coligan, John E., et al., editors. Current protocols in immunology. Vol. Chapter 7. 2007.
21. Jahrsdorfer B, Blackwell SE, Wooldridge JE, Huang J, Andreski MW, Jacobus LS, et al. B-chronic lymphocytic leukemia cells and other B cells can produce granzyme B and gain cytotoxic potential after interleukin-21-based activation. Blood. 2006; 108:2712–2719. [PubMed: 16809616]
22. Benichou, A.; Garti, N. Double Emulsions for Controlled-release Applications-Progress and Trends. CRC Press; 2001. p. 409-442.
23. Chakravarthi SS, De S, Miller DW, Robinson DH. Comparison of anti-tumor efficacy of paclitaxel delivered in nano- and microparticles. Int J Pharm. 2010; 383:37–44. [PubMed: 19747969]
24. Yoo HS, Lee KH, Oh JE, Park TG. In vitro and in vivo anti-tumor activities of nanoparticles based on doxorubicin-PLGA conjugates. J Control Release. 2000; 68:419–431. [PubMed: 10974396]
25. Hempel G, Flege S, Wurthwein G, Boos J. Peak plasma concentrations of doxorubicin in children with acute lymphoblastic leukemia or non-Hodgkin lymphoma. Cancer Chemother Pharmacol. 2002; 49:133–141. [PubMed: 11862427]
26. Makkouk A, Joshi VB, Wongrakpanich A, Lemke CD, Gross BP, Salem AK, et al. Biodegradable Microparticles Loaded with Doxorubicin and CpG ODN for In Situ Immunization Against Cancer. AAPS J. 2015; 17:184–193. [PubMed: 25331103]
27. Sawyers CL, Abate-Shen C, Anderson KC, Barker A, Baselga J, Berger NA, et al. Committee ACPRW. AACR Cancer Progress Report 2013. Clin Cancer Res. 2013; 19(20 Suppl):S4–S98. [PubMed: 24045178]
28. Silva JM, Videira M, Gaspar R, Preat V, Florindo HF. Immune system targeting by biodegradable nanoparticles for cancer vaccines. J Control Release. 2013; 168:179–199. [PubMed: 23524187]
29. Oyewumi MO, Kumar A, Cui Z. Nano-microparticles as immune adjuvants: correlating particle sizes and the resultant immune responses. Exp Rev Vaccines. 2010; 9:1095–1107.
30. Sheng Sow H, Mattarollo SR. Combining low-dose or metronomic chemotherapy with anticancer vaccines: A therapeutic opportunity for lymphomas. Oncoimmunology. 2013; 2:e27058. [PubMed: 24498564]
31. Shurin GV, Tourkova IL, Shurin MR. Low-dose chemotherapeutic agents regulate small Rho GTPase activity in dendritic cells. J Immunother. 2008; 31:491–499. [PubMed: 18463535]
32. Casares N, Pequignot MO, Tesniere A, Ghiringhelli F, Roux S, Chaput N, et al. Caspase-dependent immunogenicity of doxorubicin-induced tumor cell death. J Exp Med. 2005; 202:1691–1701. [PubMed: 16365148]
33. Ghiringhelli F, Apetoh L, Tesniere A, Aymeric L, Ma Y, Ortiz C, et al. Activation of the NLRP3 inflammasome in dendritic cells induces IL-1beta-dependent adaptive immunity against tumors. Nat Med. 2009; 15:1170–1178. [PubMed: 19767732]
34. Weinberg AD, Morris NP, Kovacsovics-Bankowski M, Urba WJ, Curti BD. Science gone translational: the OX40 agonist story. Immunol Rev. 2011; 244:218–231. [PubMed: 22017441]
35. Redmond WL, Linch SN, Kasiewicz MJ. Combined targeting of costimulatory (OX40) and coinhibitory (CTLA-4) pathways elicits potent effector T cells capable of driving robust antitumor immunity. Cancer Immunol Res. 2014; 2:142–153. [PubMed: 24778278]
36. Timar J, Ladanyi A, Forster-Horvath C, Lukits J, Dome B, Remenar E, et al. Neoadjuvant immunotherapy of oral squamous cell carcinoma modulates intratumoral CD4/CD8 ratio and tumor microenvironment: a multicenter phase II clinical trial. J Clin Oncol. 2005; 23:3421–3432. [PubMed: 15908653]
37. Brody JD, Ai WZ, Czerwinski DK, Torchia JA, Levy M, Advani RH, et al. In situ vaccination with a TLR9 agonist induces systemic lymphoma regression: a phase I/II study. J Clin Oncol. 2010; 28:4324–4332. [PubMed: 20697067]
38. Mangsbo SM, Sandin LC, Anger K, Korman AJ, Loskog A, Totterman TH. Enhanced tumor eradication by combining CTLA-4 or PD-1 blockade with CpG therapy. J Immunother. 2010; 33:225–235. [PubMed: 20445343]

39. Demento SL, Cui W, Criscione JM, Stern E, Tulipan J, Kaech SM, et al. Role of sustained antigen release from nanoparticle vaccines in shaping the T cell memory phenotype. Biomaterials. 2012; 33:4957–4964. [PubMed: 22484047]

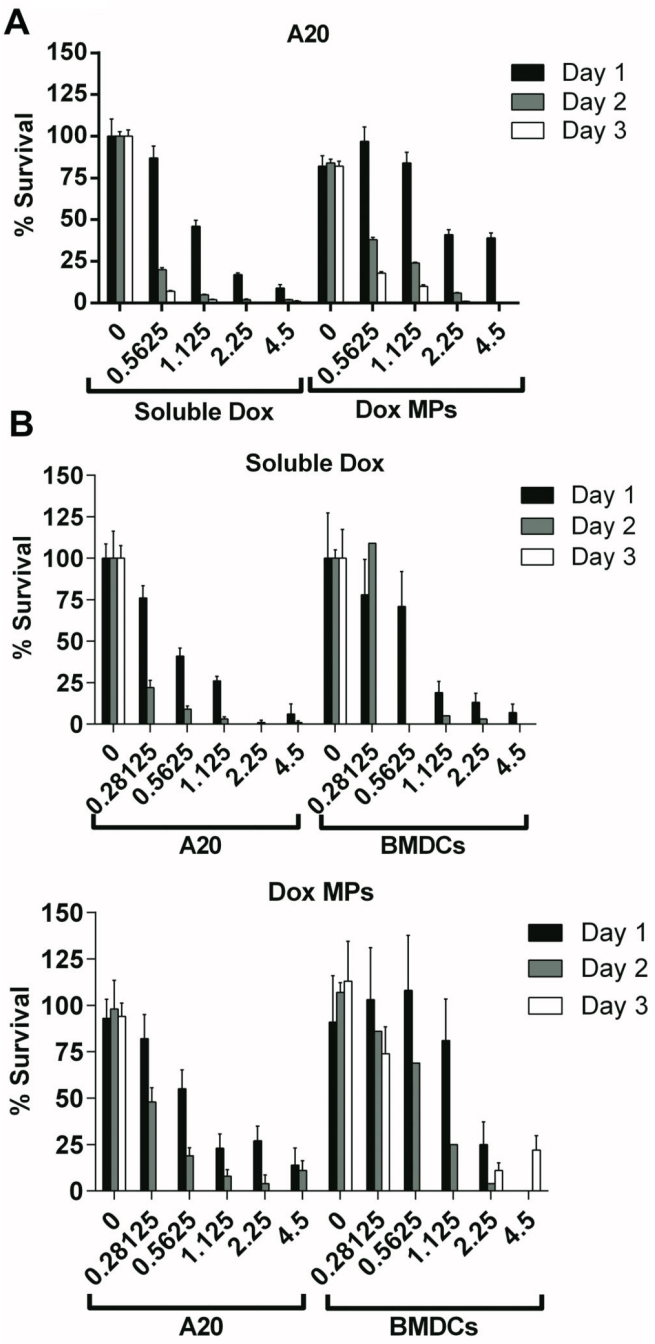

Figure 1. Dox MPs kill tumor cells more slowly than soluble Dox and are less cytotoxic to DCs

A20 B lymphoma tumor cells (**1A** and **1B**) and DCs (**1B**) were cultured for 24, 48 and 72 h with increasing concentrations (μg/mL) of soluble Dox or Dox MPs. Media or blank MPs (equivalent weight) were used as controls. Viability was assayed by MTS. Percent survival was expressed as the ratio of absorbance of treated cells relative to that of untreated cells (after subtracting the absorbance of the blank from each) multiplied by 100. Wells with equivalent MP concentrations in absence of cells were used as blanks. Results are mean ± SEM (n = 4).

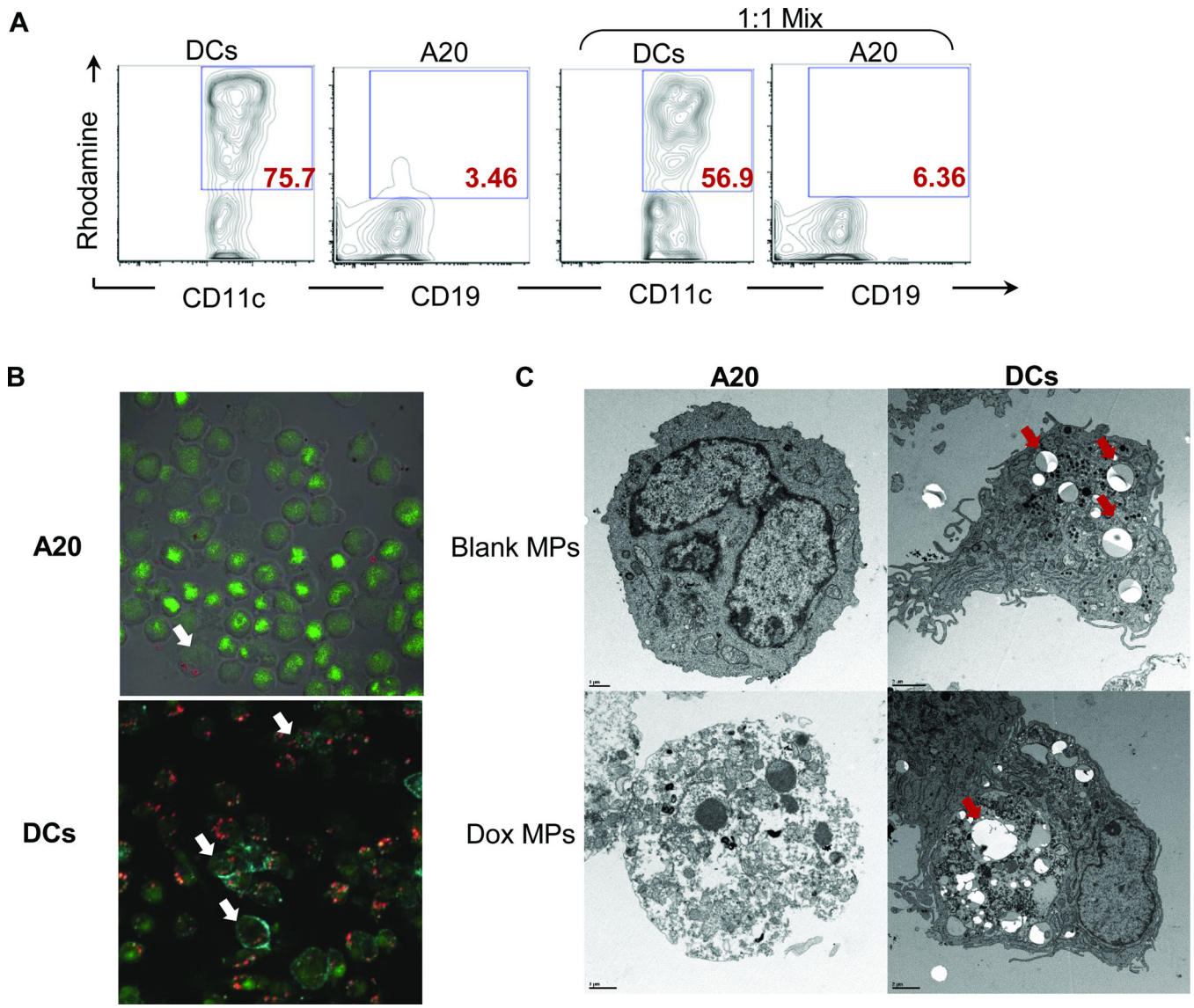

Figure 2. Dox MPs do not require internalization by tumor cells for their cytotoxic activity

2A. A20 and DCs were cultured alone or in a 1:1 mix with rhodamine-loaded MPs for 24 h. Uptake was assessed by flow cytometry by gating on Rhodamine^{+} BMDCs (CD11c^{+}) and A20 (CD19^{+}). Representative flow plots are shown. **2B.** A20 were cultured for 24 h with no treatment or with Dox MPs at a final Dox concentration of 2.25 μg/mL. Cells were washed, stained with Cyto-16 (nucleic acid dye), cytospun and visualized by confocal microscopy. DCs were similarly treated, stained with Cyto-16 and anti-CD11c, and visualized. Representative images of Dox MP treatment are shown (×400) (Green = Nucleic acid; Blue = CD11c; Red = Dox). White arrows point to cells with internalized Dox MPs. **2C.** A20 and DCs were cultured for 24 h with no treatment or with blank MPs (equivalent weight) or Dox MPs at a final Dox concentration of 1 μg/mL. Cells were washed, fixed and analyzed by TEM. Representative images for blank MP and Dox MP treatments are shown. Red arrows point to MPs (scale bar: 1 μm for A20 and 2 μm for DCs).

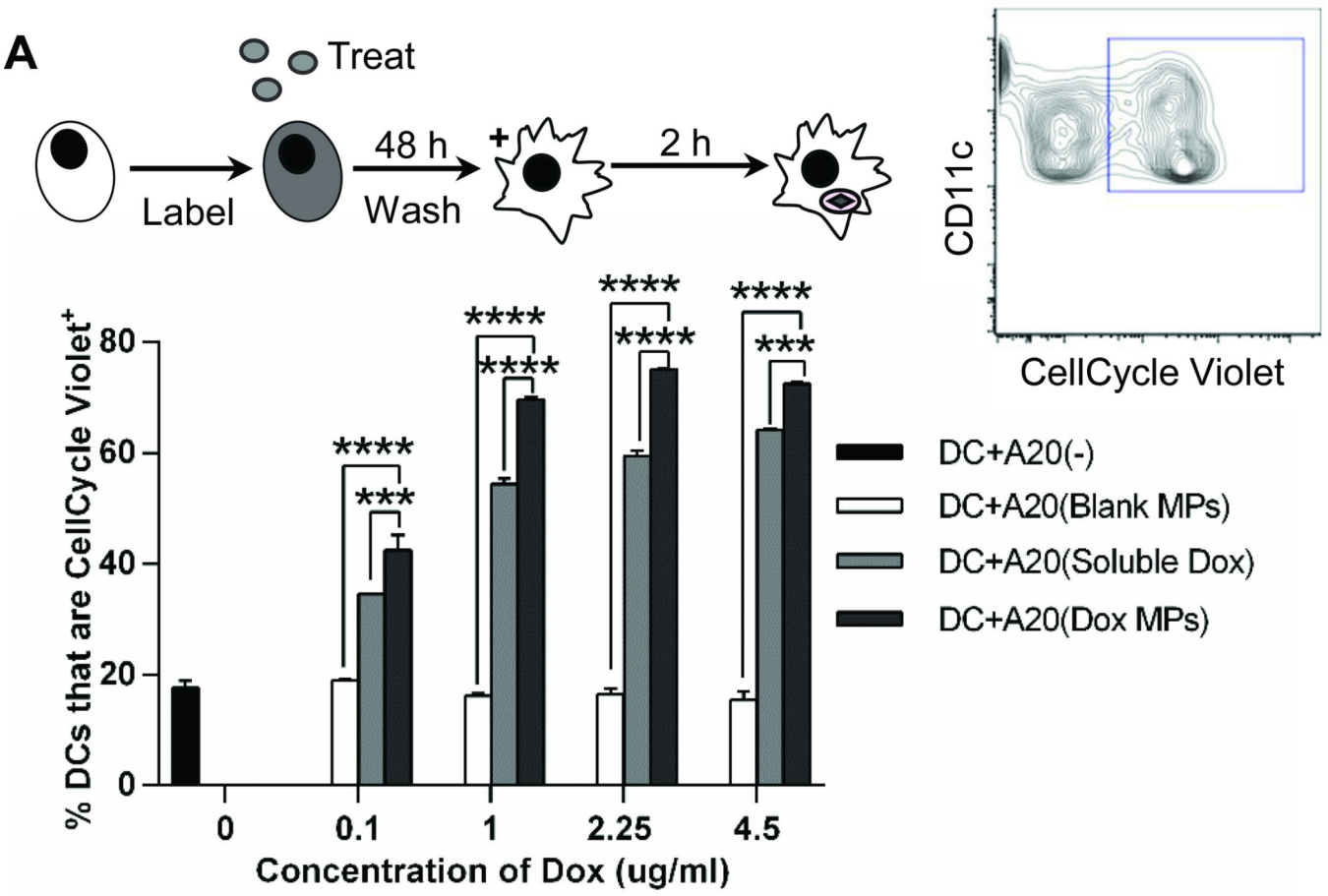

Figure 3. Dox MPs enhance phagocytosis of tumor cells by DCs

A20 were labeled with CellCycle Violet then left untreated or treated with soluble Dox, blank MPs or Dox MPs for 48 h. Cells were washed, co-incubated with DCs (1:1 ratio) for 2 h, stained for CD11c and evaluated by flow cytometry. Cells were gated on $CD11c^+$ CellCycle $Violet^+$. Results are mean ± SEM (n = 2). *** $p<0.001$; **** $p<0.0001$.

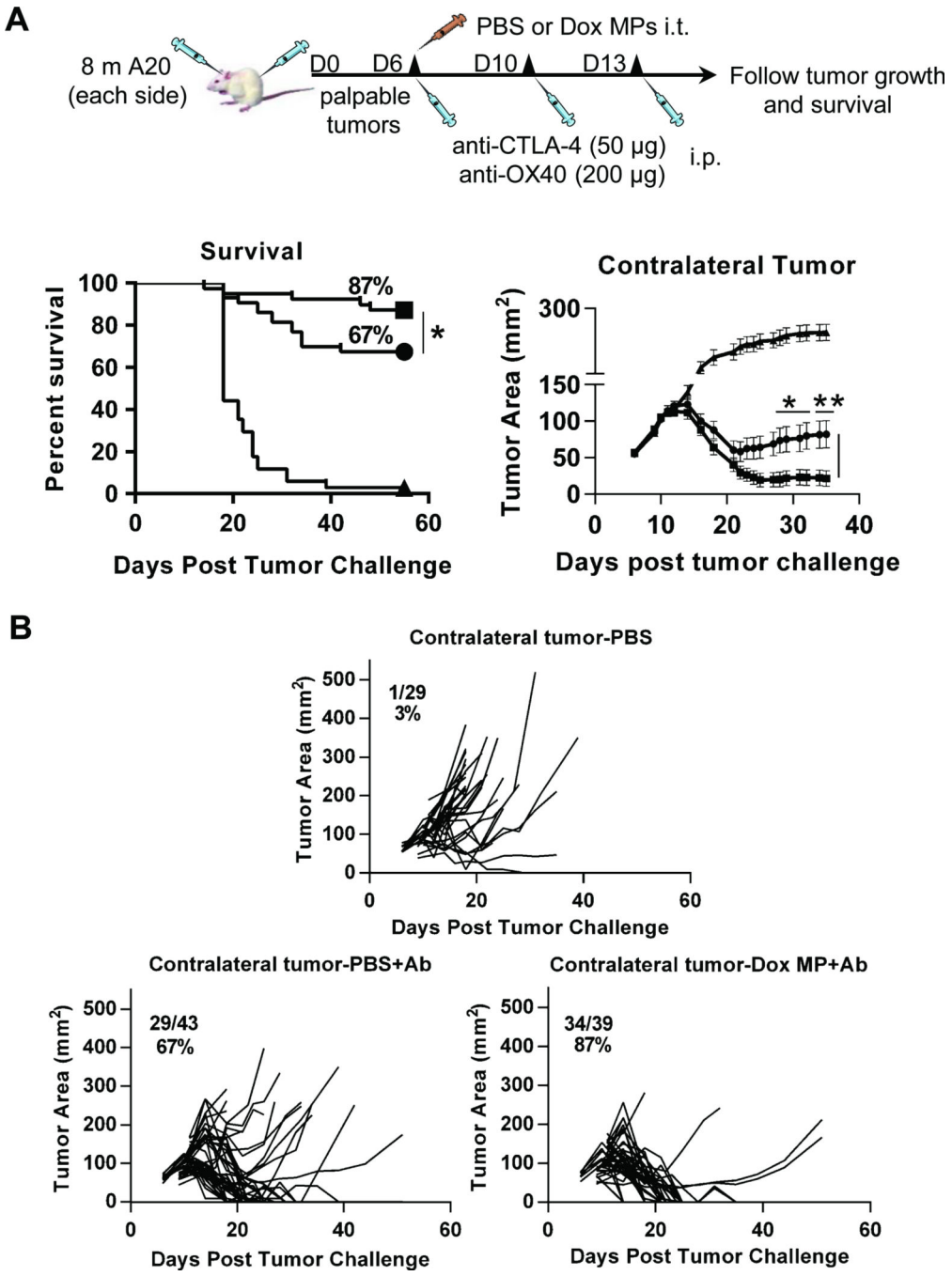

Figure 4. Three-step therapy eradicates distant tumors and enhances survival

4A. Eight million A20 cells were injected subcutaneously into each flank of BALB/c mice (6–12/group). Treatment began when tumors reached 5–7 mm in largest diameter (typically between days 6 and 11). Left-side tumors were injected with PBS or Dox MPs (2 μg Dox). Mice also received three intraperitoneal injections of anti-CTLA-4 (50 μg) and anti-OX40 (200 μg) over 10 days (collectively referred to as Ab). The systemic antitumor immune response was assessed by measuring the size of the contralateral tumor and disease-free survival. Tumor areas are mean ± SEM. Data shown are pooled from four independent

experiments. * $p<0.05$; ** $p< 0.01$. **4B.** Spider plots representing tumor size for individual mice per group. Fractions and percentages represent mice that were tumor-free at Day 55 post tumor challenge. Symbols: Triangle (PBS); circle (PBS+Ab); and square (Dox MP +Ab).

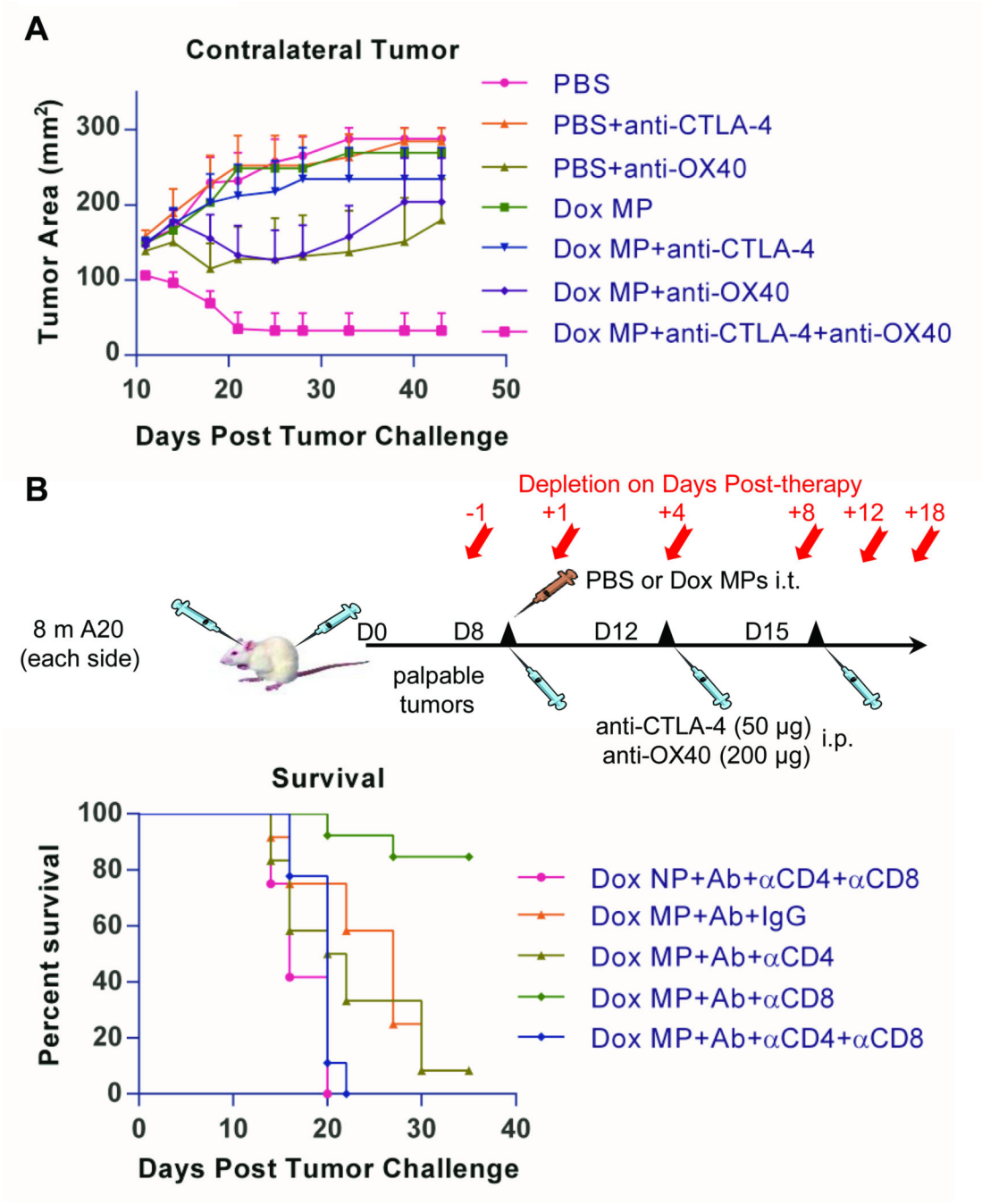

Figure 5. Three-step therapy induces CD4- and CD8-dependent immune responses and requires all therapy components for maximum efficiency

5A. Mice (7–8/group) were treated and observed similarly to that described for Figure 4 except that different combinations among the three therapy components were used to observe the contribution of each. Tumor areas are mean + SEM. **5B.** Mice (9–13/group) were treated and observed as before. Treatments consisted of PBS as control or Dox MP +Ab. Mice receiving three-step therapy additionally received multiple injections of either anti-CD4, anti-CD8, or both according to the schematic shown.

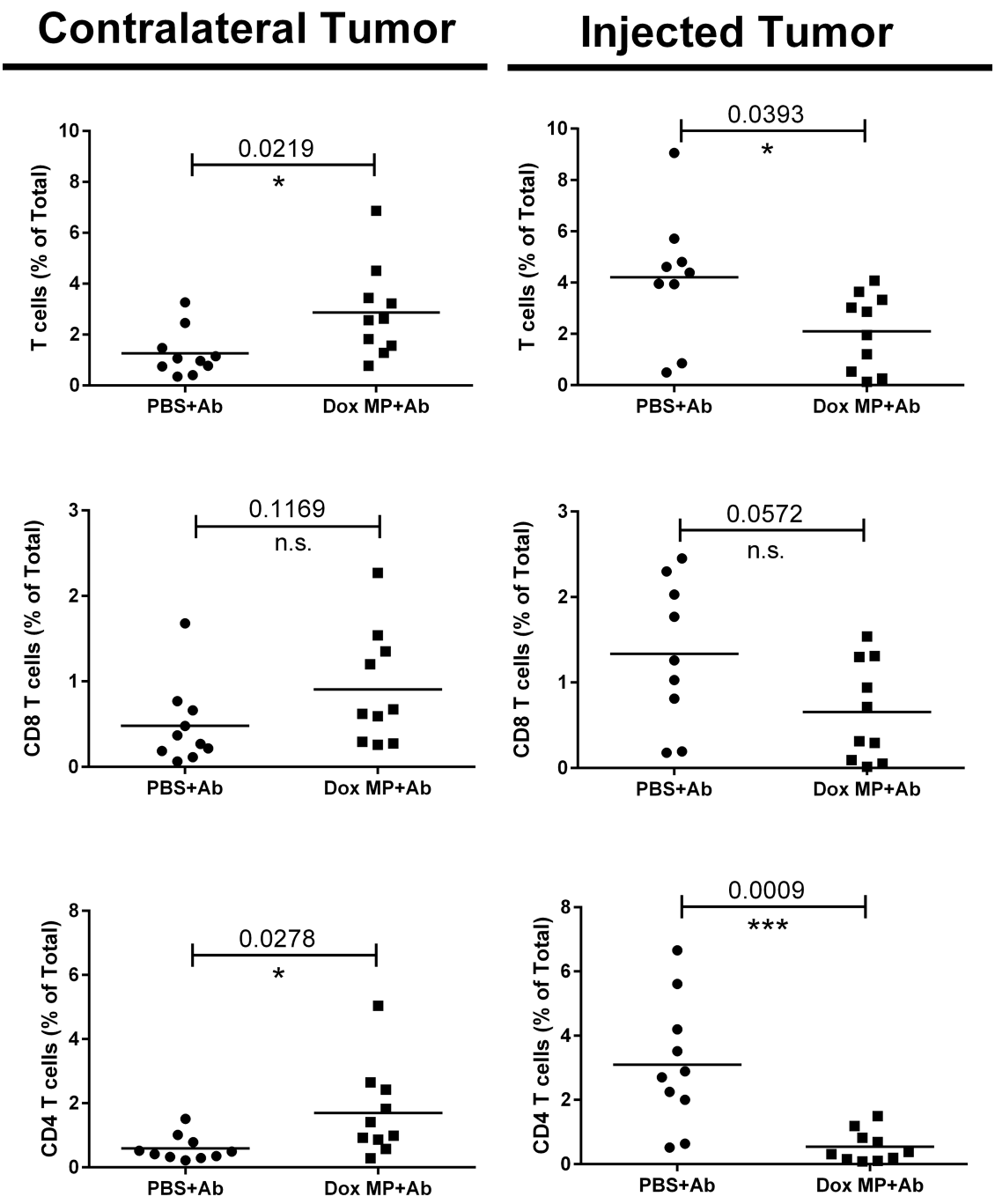

Figure 6. Three-step therapy enhances T-cell infiltration into contralateral tumors

Mice (5/group) were treated as before. Treatments consisted of PBS+Ab or Dox MP+Ab. On Day 5 post therapy, injected and contralateral tumors were harvested and T-cell infiltrates were analyzed by flow cytometry. Results are presented as percentages of total tumor cells. Data shown are pooled from two independent experiments. * $p<0.05$; *** $p<0.001$. n.s. not statistically significant.

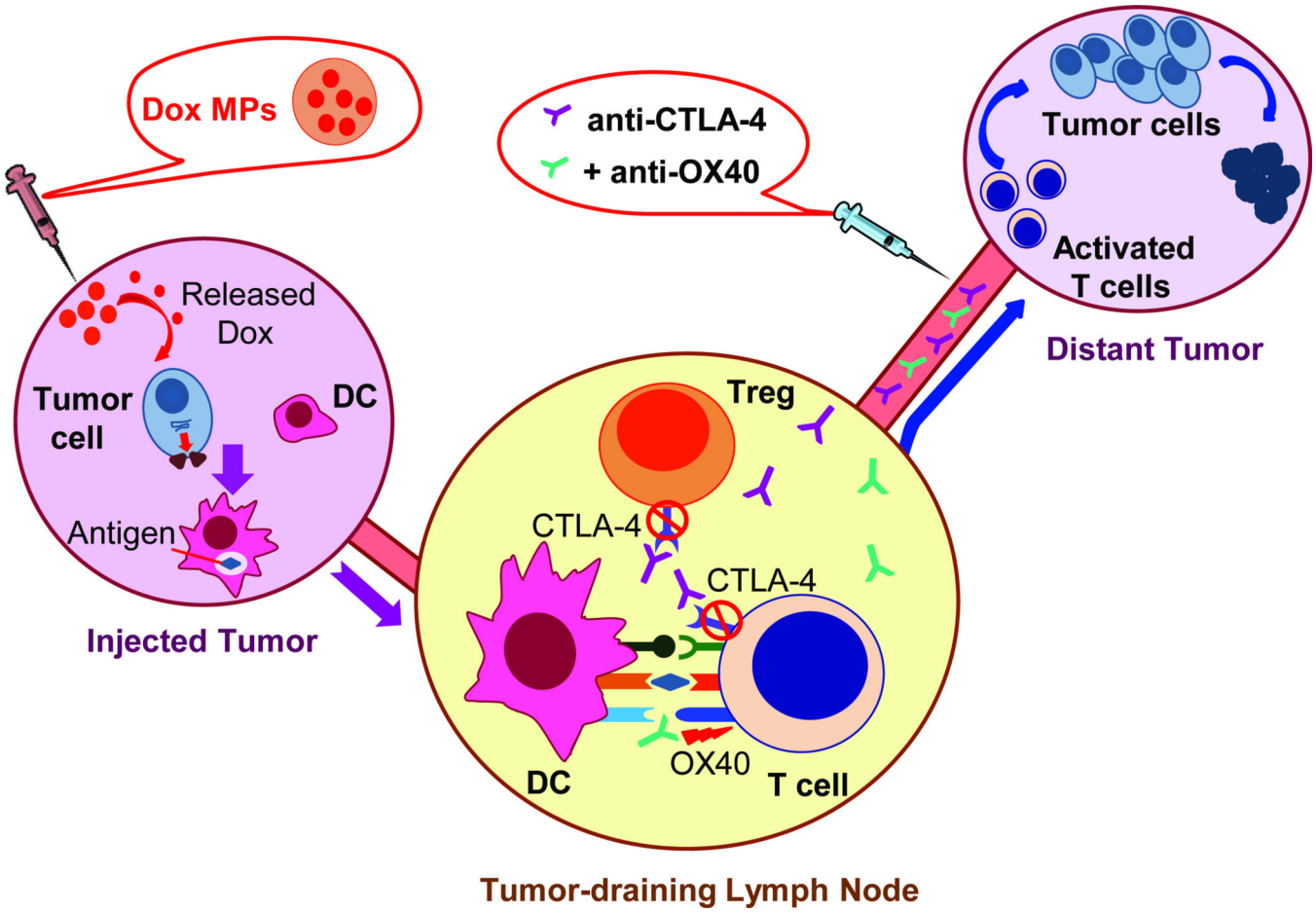

Figure 7. A systemic immune response is generated through local tumor manipulation- a proposed schematic

Dox MPs injected intratumorally upregulate surface calreticulin expression on dying tumor cells, enhancing their phagocytosis by DCs which migrate to draining lymph nodes and present tumor antigen to antigen-specific T cells. Anti-OX40 enhances T-cell activation while anti-CTLA-4 blocks immunosuppression imposed by CTLA-4, thus allowing tumor-specific T cells to proceed unrestrained to distant tumor sites.